Stiff clay c' ϕ' derivation through pressuremeter test data

T. L. Gouw
Universitas Katolik Parahyangan, Bandung, Indonesia, gtloffice@gmail.com

ABSTRACT: Due to its rather brittle nature, retrieving undisturbed samples of Jakarta cemented greyish stiff clay, often found at a depth of 30 to 120m, is very difficult. Good and reliable shear strength parameters, i.e, c and ϕ values, obtained from triaxial test are hardly available. In practice, many engineers are often forced to estimate these parameters through SPT test data which are of course greatly varied from one engineer to another. It will be good if these parameters can be derived by an in-situ testing device. Since pressuremeter is an in-situ soil testing device able to yield stress strain relationship of soil, a research is carried out to derive c and ϕ values from pressuremeter test data curves through cavity expansion theory. Results prove that c and ϕ values of Jakarta stiff clay can be derived by matching pressuremeter test data curve with values calculated through modified cavity expansion theory. The derived c and ϕ values are comparable with CIU triaxial test strength parameter obtained from relatively good 'undisturbed' samples.

Keywords: Jakarta stiff clay; shear strength; pressuremeter; cavity expansion theory

1. Introduction

The first 30m depth of Jakarta alluvial coastal plain generally consists of alternating soft to medium silty clay and loose to medium dense sands layers. Below 30m and up to 60m depth, alternating old alluvium deposits of cemented stiff clay and cemented sands are found. Below 60m depth, the soil generally consists of stiff cemented old alluvium clay. The cemented stiff clay layer exhibits a rather brittle nature. It needs a highly skillful technician to get and to prepare good quality of undisturbed samples for triaxial test. Many soil laboratory does not have such qualified person, therefore, engineers are often 'forced' to estimate its c and ϕ values, as well as its stiffness value through SPT data which is of course can greatly varied from one engineer to another as SPT test itself is often far from reliable when executed on clayey soils. It is good if these parameters can be derived by means of another more reliable in-situ test. Since pressuremeter test is so far the only in-situ testing device able to generate a stress strain curve of in-situ soils, it hypothesis that by simulating the pressuremeter test through cylindrical cavity expansion theory and matching the resulting stress strain curve with the actual test data curve, it is possible to calculate the shear strength parameters, i.e., c and ϕ values. An in-depth research is the carried out to investigate this possibility. The methodology and the result of the research are presented in this paper.

2. Literature Reviews

2.1. Pressuremeter test

Pressuremeter test, originally developed by Louis Ménard in 1957 (Baguelin et al [1-2]; Gambin [3]), is performed by lowering a cylindrical probe into a carefully prepared borehole to the required test depth where the cylindrical membrane is then pressurized against the borehole wall and the subsequent volume expansion of the cylindrical membrane is measured.

Generally, the pressure is applied by pumping de-aired water into the cylindrical membrane and its volume of expansion is measured through the volume pumped into the membrane. The actual pressure or stress working against the borehole wall is corrected against the membrane resistance and against the hydrostatic pressure from the manometer to the centre of the membrane. The volume of expansion is corrected against the expansion of the hose to deliver the water from the control unit to the membrane (ASTM D4719-00 [4]). The corrected volume is then converted into radial strain of the borehole wall. The resulting corrected radial stress strain curve acting against the soil can then be plotted. Fig. 1 shows the schematic pressuremeter test device and the typical test data curve modified after Briaud [7].

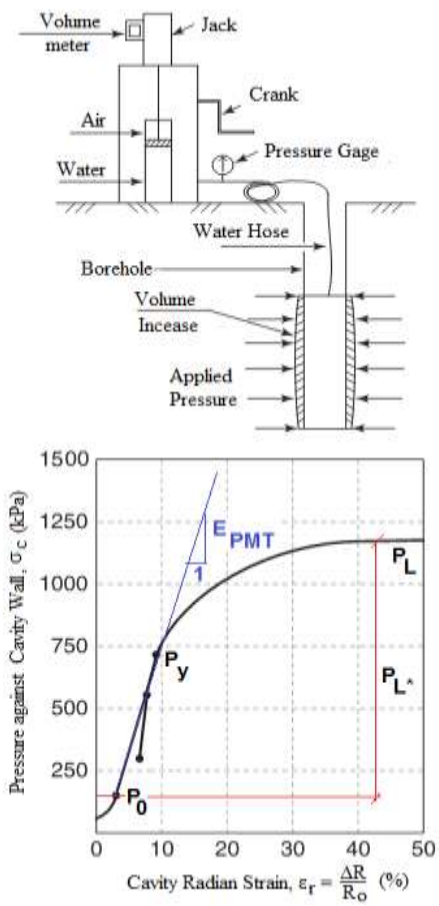

Figure 1. Pressuremeter test and typical test graph modified after Briaud [7]

From the installation point of view, there are three types of pressuremeter, i.e.: preborehole pressuremeter, push-in pressuremeter, and self-boring pressuremeter (Baguelin et al [2]; Clayton et al [6]; Briaud [7]; Clarke [8]).

Preborehole pressuremeter is performed on a carefully prepared borehole prior to the insertion of the test probe. Push-in pressuremeter probe is equipped with a conical tip and the probe is pushed into the soil to the test depth before the test is begun. Self-boring pressuremeter probe is equipped with a drilling bit at its tip, the probe is advanced into the ground following the drilling process. Push-in pressuremeter induces more disturbances to the borehole wall than pre-borehole pressuremeter, self-boring pressuremeter induces less disturbances.

Among those three types, pre-borehole pressuremeter has been employed in Indonesia as early as 1983 (Gouw [9]) and up to now it is the most commonly adopted. Push-in pressuremeter is never applied, and only one government institution has self-boring pressuremeter but rarely used. Therefore, the research is limited to pre-borehole pressuremeter test data only.

2.2. Pressuremeter parameters

From the stress strain pressuremeter test curve, traditionally six parameters are generated, those are: P_o, P_y, P_L, K_m, E_m, and G as elaborated below:

2.2.1. Horizontal pressure, P_o

Horizontal pressure, P_o, is defined as the pressure where the membrane first touches the borehole wall, i.e. first point at the beginning of linear or elastic part of pressuremeter stress strain curve, indicated as P_o in Fig.1. This pressure is also often interpreted as total horizontal pressure at rest as represented in the equation below,

$$P_o = \sigma'_{vo} k_o + u_o \quad (1)$$

$$\sigma'_{ho} = \sigma'_{vo} k_o = P_o - u_o \quad (2)$$

Where σ'_{vo} is vertical effective pressure, σ'_{ho} is horizontal effective pressure, k_o is at rest horizontal earth pressure coefficient, u_o is hydrostatic groundwater pressure.

2.2.2. Yield pressure, P_y

The end of the linear part and the beginning of the non-linear (plastic) part of the pressuremeter test curve, indicated as P_y in Fig. 1.

2.2.3. Limit pressure, P_L

Limit pressure, indicated as P_L in Fig. 1, is defined as the ultimate horizontal pressure of pressuremeter test curve where soil start to 'flow', i.e. radial strain keeps on increasing while the pressure is hardly increases. Generally, in real test, this limit pressure is hardly achieved, and the test curve must be extrapolated in a logaritmic plot as shown in Fig. 2.

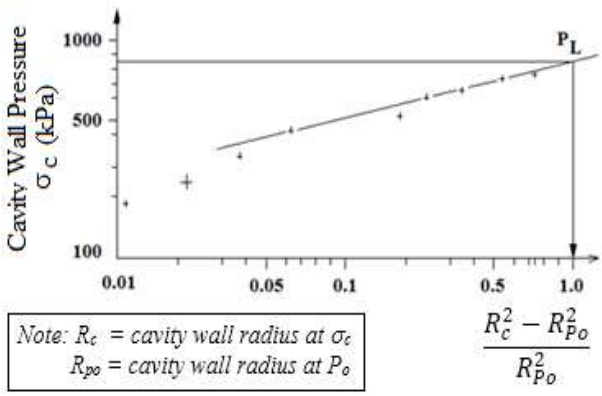

Figure 2. Extrapolation of test data to get P_L (modified after Baguelin et al [2] and Ghionna et al [10])

2.2.4. Coefficient of horizontal subgrade reaction, K_m

Coefficient of horizontal subgrade reaction, K_m, is obtained through linear part of the test curve, i.e.:

$$K_m = \frac{\Delta P}{\Delta R} = \frac{P_y - P_o}{R_{Py} - R_{Po}} \quad (3)$$

Where R_{Py} and R_{Po} is cavity radius at yield pressure P_y and horizontal pressure, P_o, respectively.

2.2.5. Stiffness or deformation modulus, E_m

Soil stiffness modulus, E_m, is derived by the following equation:

$$E_m = (1+\upsilon)\ \frac{R_{Po}+R_{Py}}{2}\ K_m \quad (4)$$

Where v is Poisson ratio of the soil, usually taken as 0.33.

2.2.6. Shear modulus, G

Shear modulus, G, is calculated as follows:

$$G = \frac{E_m}{2(1+\upsilon)} \quad (5)$$

2.2.7. Shear strength parameters

Other than those traditional pressuremeter parameters, some researchers derive undrained shear strength of clays and angle of internal friction of sands. Gibson and Anderson [11], formulized undrained shear strength of cohesive soils, S_u, through Tresca constitutive model as follows:

$$\sigma_c = \sigma_{ho} + S_u \left[1 + ln\left(\frac{G}{S_u}\right) + ln\left(\frac{\Delta V}{V}\right)\right] \quad (6)$$

Where σ_c is pressuremeter cavity wall pressure, σ_{ho} is total horizontal stress of the soil, $\Delta V/V = Ln\left[\left({R_c}^2 - {R_{Po}}^2\right)/R_c\right]$= volumetric strain, R_c is the cavity wall radius at σ_c.

With Eq. (6), Gibson and Anderson indicated that if σ_c is plotted against $ln(\Delta V/V)$, the plastic part of the test

data will form a straight line, and the slope of this straight line is the undrained shear strength of the soil as show in Fig.3.

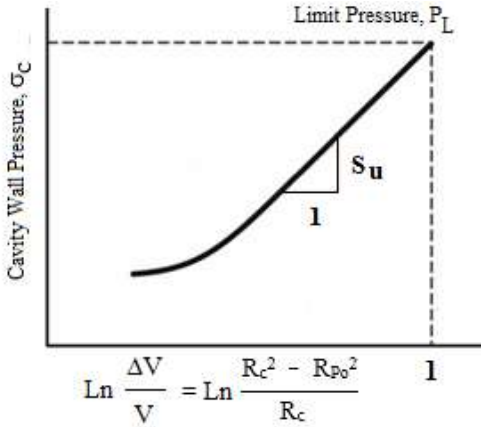

Figure 3. Derivation of undrained shear strength, S_u (modified after Gibson and Anderson [11])

Marshland and Randolph [12] derived a simpler formula to derived the undrained shear strength, S_u:

$$S_u = (P_L - P_o) / N_P \tag{7}$$

Where N_p is a constant taken as 6.2. Mair and Wood [13] reported that Eq. (7) is less sensitive against the effect of pressuremeter installation method. Mair and Wood [13], Windle and Wroth [14-15], reported that generally undrained shear strengths derived from pressuremeter test were higher than laboratory test data.

Some researchers have also tried to derive angle of internal friction of sands through pressuremeter test data (Hughes et al [16]; Fahey and Randolph [17]; Mair and Wood [13]; Schnaid [18]). As in undrained shear strength case, the resulting friction angles were also higher than the ones obtained from triaxial tests (Bruzzi et al [19]). However, from literatures published up to 2013, it seems that no attempt has been tried to derive the effective shear strength c‘ and ϕ‘ of clayey soils by using pressuremeter test data. In France, where pressuremeter is widely used, the engineers directly adopted the pressuremeter parameters E_m, G, P_y and P_L to calculate foundation capacity and settlement (Baguelin et al [2]; Gambin [20]; Boumedi et al [21]; Bustamante et al [22]; Gambin and Frank [23]; Reiffsteck [24]; Schlosser et al [25]; Hamidi et al [26]).

Outside French, the research generally directed to derive and to use undrained shear strength (Briaud et al [27]; Jefferies [28]; Ferreira and Robertson [29]; Briaud [30]; Bullock [31]; Silvestri and Ghassan [32]; Ramdane et al [33]). Only one literature is found trying to estimate c‘ and ϕ‘ values of clayey soils by using pressuremeter test data through cavity expansion theory by Mecsi [34]. The cavity expansion theory and Mecsi model is elaborated below.

2.3. Cylindrical cavity expansion theory

Cylindrical cavity expansion theory discussed the change of stresses, pore water pressure and deformation of soils caused by expansion or contraction of cylindrical cavity. This theory has been widely employed in analysing deep foundation, tunnels, borehole stability, stone columns and other geotechnical problems (Ladanyi [35]; Baguelin [1]; Vesic [36]; Vesic [37]; Baligh [38]; Wroth and Windle [39]; Datye and Nagraju [40]; Pandit et al [41]; Yu 2000 [42]).

Vesic [36] divided the expansion of cylindrical cavity into elastic and plastic zone as illustrated in Fig. 4. Based on this Vesic work and Mohr Coulomb failure criterion, Mecsi [34] derived equations to calculate the c and ϕ values of soil from pressuremeter test data. His equations are elaborated below:

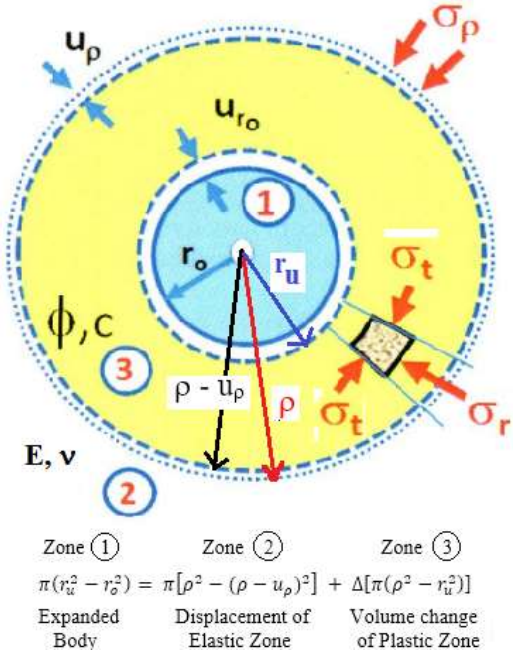

r_o = initial cavity radius; r_u = pressurised radius; ρ = radius of plastic zone; u_{ro} = cavity radial displacement; u_ρ = radial displacement of plastic zone; σ_r = radial stress; σ_t = tangential stress; σ_ρ = radial stress at boundary of plastic Zone

Figure 4. Cylindrical cavity expansion zone (modified after Mecsi [34])

$$\sigma_u = \frac{2.c}{\sqrt{\xi}} \tag{8}$$

$$\xi = \frac{1-sin\phi}{1+sin\phi} \tag{9}$$

σ_u and ξ are derived from Mohr circle as illustrated in Fig. 5.

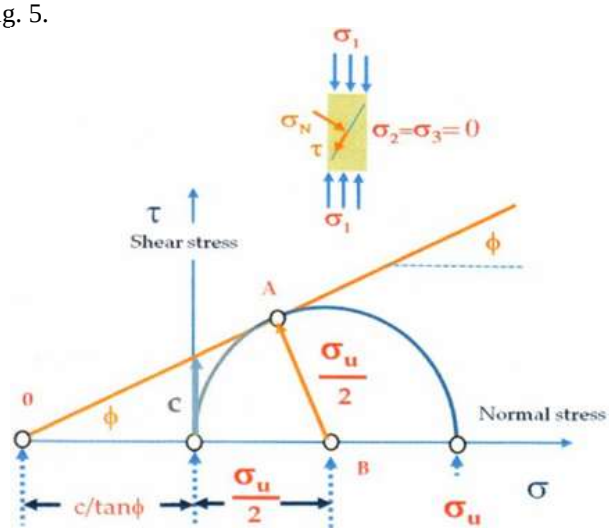

Figure 5. Definition of σ_u and ξ from Mohr failure criterion (after Mecsi [34])

The relationship of soil stiffness vs deformation modulus (soil sttiffness) is assumed to have a power function as follows.

$$E_s = E_o \left(\frac{\sigma_c}{\sigma_{ref}}\right)^a \tag{10}$$

Where E_s is the deformation modulus at a cavity pressure of σ_c, and E_o is the deformation modulus at a reference pressure σ_{ref} = 100kPa as shown in Fig. 6, a is named as rigidity index.

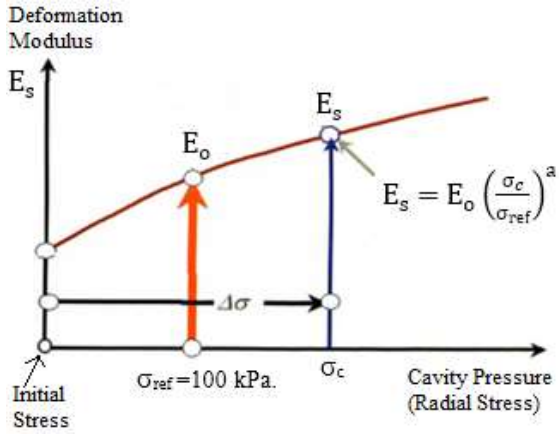

Figure 6. Deformation modulus vs cavity pressure (after Mecsi [34])

When a cylindrical cavity is subjected to a cavity pressure σ_c, the radial stress reduces from σ_c at the cavity wall to at rest horizontal earth pressure of σ'_{ho} at a certain distance. At the same time, the induced tangential stress σ_c first reduces until radius ρ, where it then increases to finally reaches σ'_{ho}. The radius where the soil is still in compression and the tangential stresses still reduces is defined as radius of compression (plastic) zone, ρ, and formulated as:

$$\rho = r_c \left(\frac{\sigma_c + c.cot\phi}{\sigma_{\rho h} + c.cot\phi}\right)^{\frac{1+sin\phi}{2sin\phi}} \tag{11}$$

Where r_c = cavity radius at cavity pressure σ_c and $\sigma_{\rho h}$ is horizontal or radial stress at boundary of compression zone which is defined as:

$$\sigma_{\rho h} \approx \frac{\sigma'_{ho}}{a}\left[1+\xi-\sqrt{(1+\xi)^2-2a(1-\xi)2a\xi\frac{\sigma_u}{\sigma'_{ho}}}\right]+\sigma'_{ho} \tag{12}$$

The radial stress inside the compression zone (at radius r ≤ ρ):

$$\sigma_r = \left(\sigma_{\rho h} + \frac{c}{tan\phi}\right).\left(\frac{\rho}{r}\right)^{\frac{2sin\phi}{1+sin\phi}} - \frac{c}{tan\phi} \tag{13}$$

The radial stress outside the compression zone (at radius r > ρ):

$$\sigma_r = \left(\sigma_{\rho h} - \sigma'_{ho}\right).\left(\frac{\rho}{r}\right)^2 + \sigma'_{ho} \tag{14}$$

The induced radial strain, ε_r:

$$\Delta\varepsilon_r = \frac{\sigma_{ref}}{(1-a)E_o}\left[\left(\frac{\sigma_r}{\sigma_{ref}}\right)^{1-a} - \left(\frac{\sigma'_{ho}}{\sigma_{ref}}\right)^{1-a}\right] \tag{15}$$

The induced radial displacement u_r:

$$\Delta u_r = \frac{\Delta\varepsilon_{r(i-1)} + \Delta\varepsilon_{r(i)}}{2}\left(r_{(i)} - r_{(i-1)}\right) \tag{16}$$

With the above formulas, it is supposed to be able to derive the c and ϕ of clayey soils by matching the pressuremeter test data curve the calculated radial strain or radial displacement, i.e. matching σ_c vs ε_r plot from pressuremeter against σ_c vs ε_r plot from the above cavity expansion formulas.

3. Field and laboratory test performed

The research was carried out at a project site at central Jakarta area, where many high-rise buildings are located. The following field and laboratory testings were carried out:

- 21 deep borings carried out between 90 to 120 m depths. SPT tests were taken at every 2 to 3.5 m intervals.
- 20 pre-borehole pressuremeter tests conducted at cemented stiff clay layers.
- A total of 123 undisturbed samples for laboratory index properties tests, triaxial UU, triaxial CIU and consolidation tests.

Fig. 7 to 15 show index and engineering properties of the soil tested. The subsoil exhibits an increasing trend of SPT blow counts against depth, and the water contents below 20m falls near the plastic limits, an indication of stiff clays (Fig. 7). Plasticity indices of the stiff clay, found below 20m depth, are mostly within 20 to 60% with liquidity indices less than 0.25 (Fig. 8). Other index properties are shown in Fig. 9 to 11.

Fig. 12 shows the compression and re-compression indices, Fig. 13 shows the pre-consolidation pressure and the undrained shear strength of the stiff clay from triaxial UU tests. The pre-consolidation pressures appear to be increasing with depth. Comparing with the corresponding effective stresses, the over consolidation ratio of the stiff clay layers if found to be around 2.0. The undrained shear strengths of the stiff clay layer are found to be increasing with depth, from around 90 kPa at 24 m depth to about 300 kPa at 100 m depth. The effective and total shear strength obtained from triaxial CIU tests are shown in Fig. 14 and 15. Fig. 16 shows typical graphs of pressuremeter test performed. Fig. 17 shows a bad quality pressuremeter test data where the hole is too large.

Note that the notation of PMT DB-xx/yy in the pressuremeter graphs mean pressuremeter test (PMT) conducted at borehole no xx at depth of yy meter.

Fig. 18 shows the parameters derived from the pressuremeter tests. The notations on the graphs are as defined before, whereas E_{ur} means unloading-reloading deformation modulus derived from the test. Fig. 19 shows the soil effective horizontal stress σ'_{ho} is obtained by subtracting pressuremeter total horizontal pressure P_o, with its corresponding hydrostatic groundwater pressure, as formulated in Eq. (1). It is important to observe the profile of effective horizontal stress as it needs to be implemented in Eq. (12), Eq. (14), and Eq. (15).

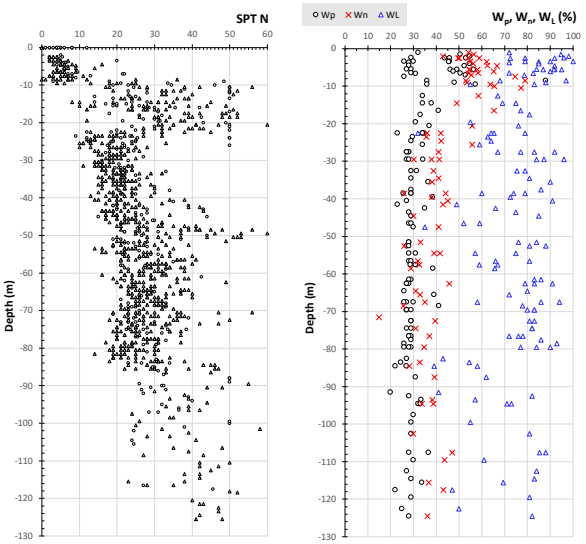

Figure 7. SPT blow counts and Atterberg Limits

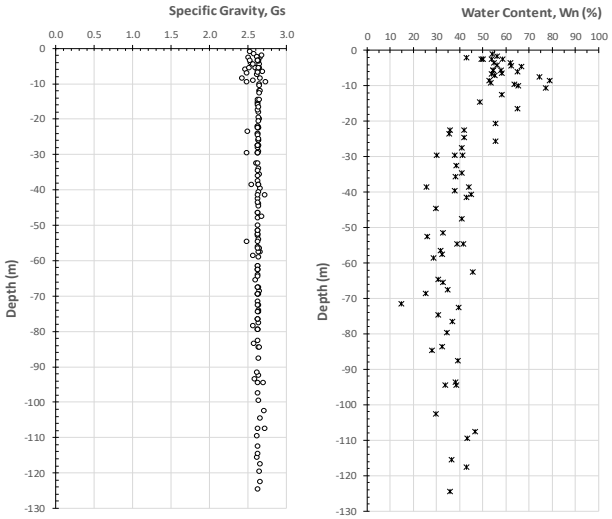

Figure 10. Specific gravity and water content

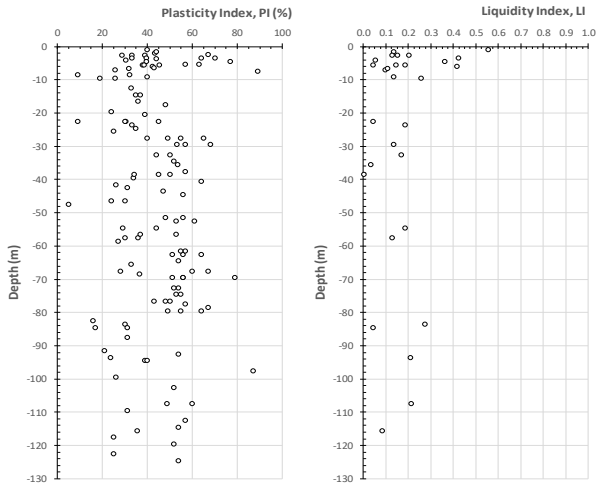

Figure 8. Plasticity and liquidity indices

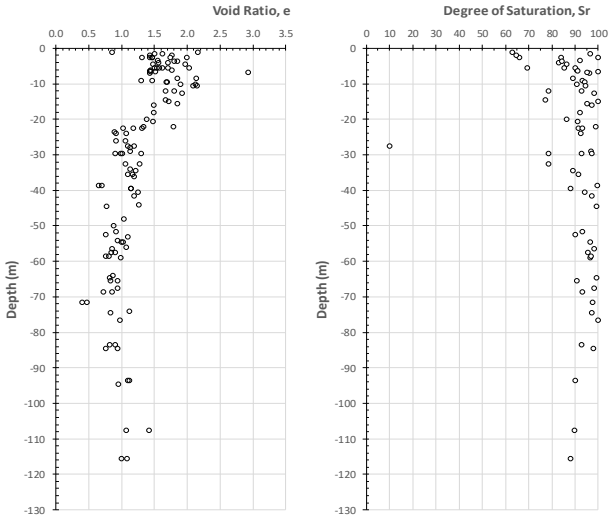

Figure 11. Void ratio and degree of saturation

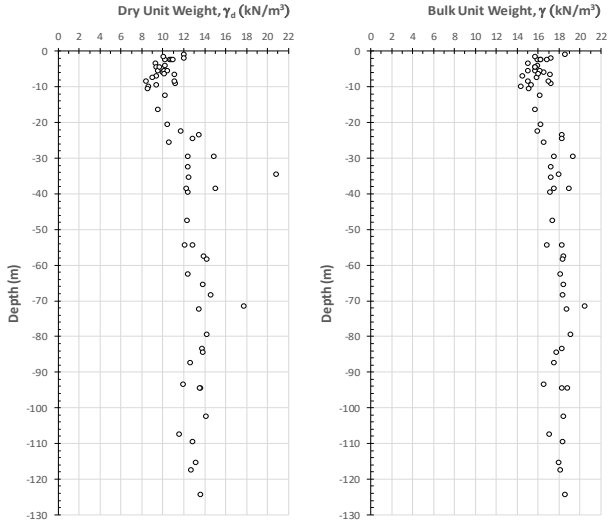

Figure 9. Dry and bulk unit weight

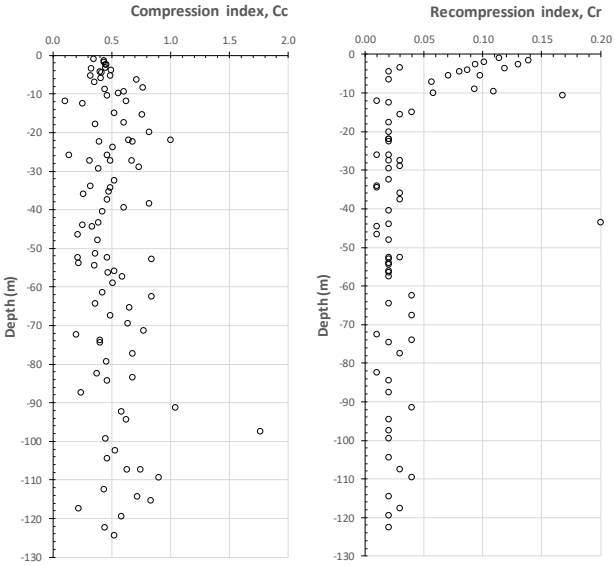

Figure 12. Compression and recompression indices

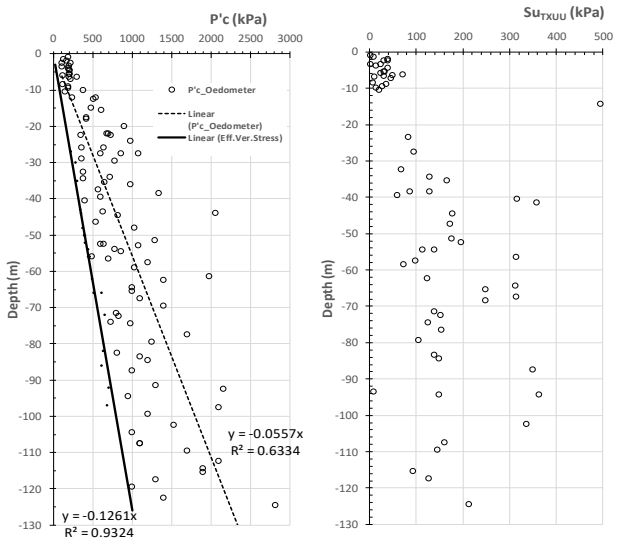

Figure 13. Pre-consolidation pressure and undrained strength

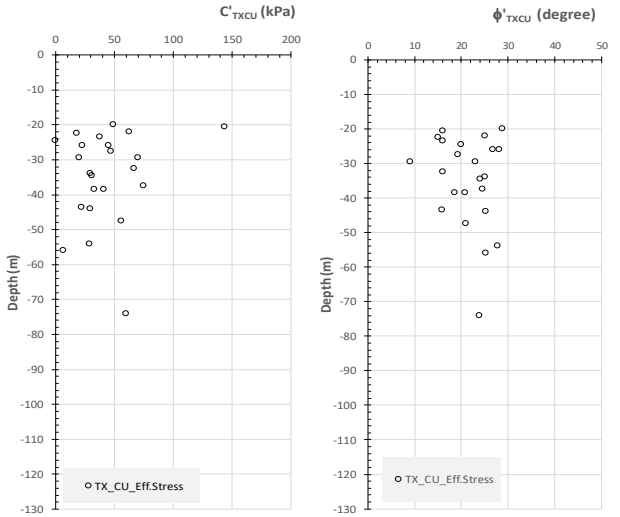

Figure 14. c' and ϕ' from triaxial CIU tests

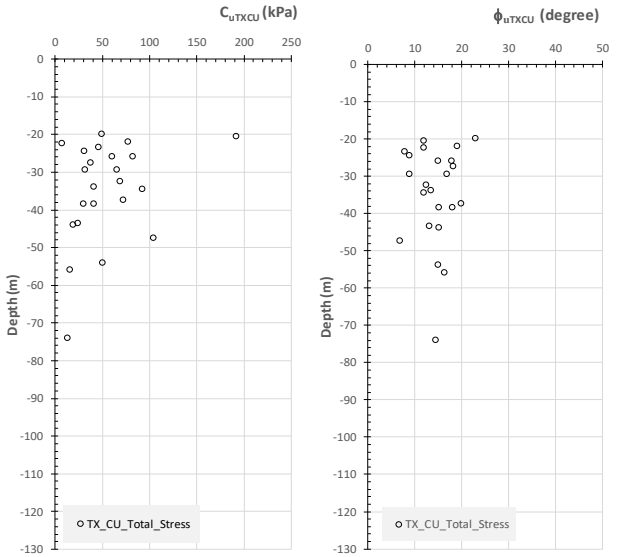

Figure 15. c_u and ϕ_u from triaxial CIU tests

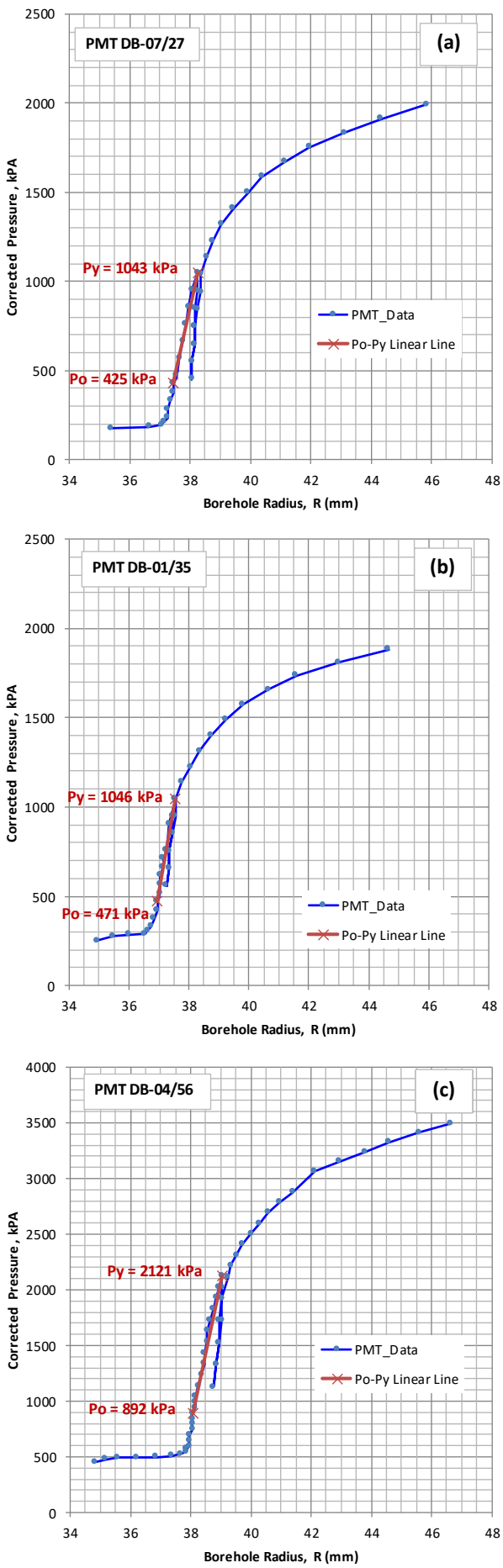

Figure 16. Good pressuremeter test graphs

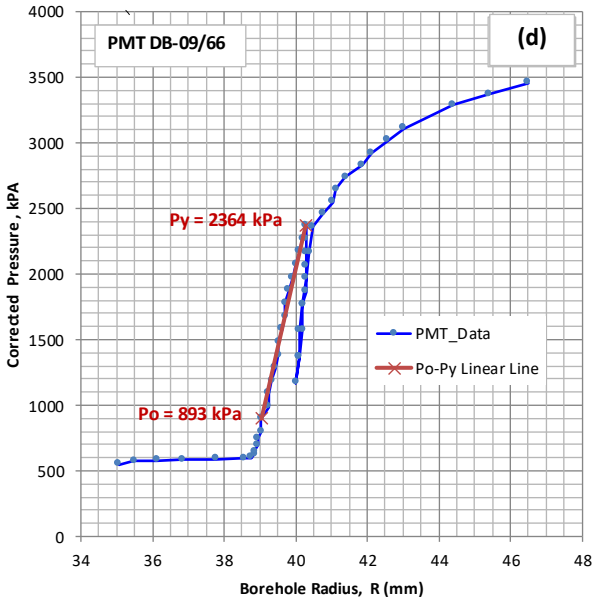

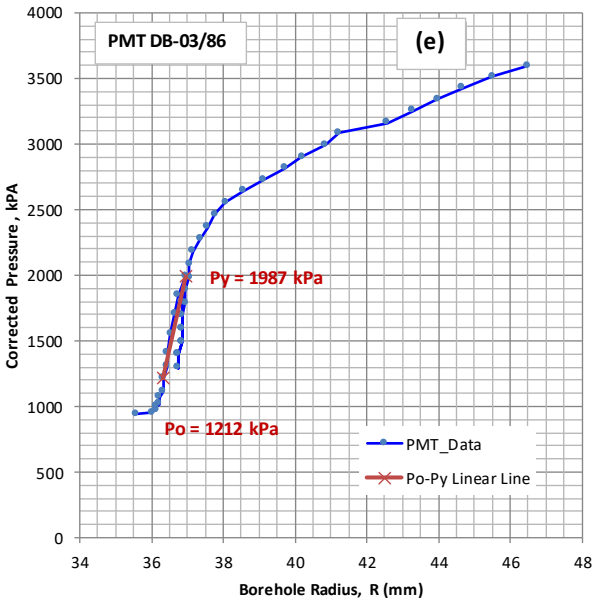

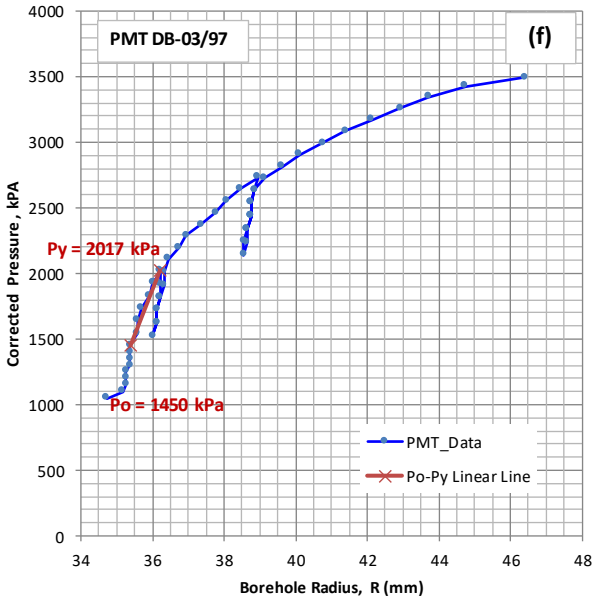

Figure 16. Good pressuremeter test graph (con't)

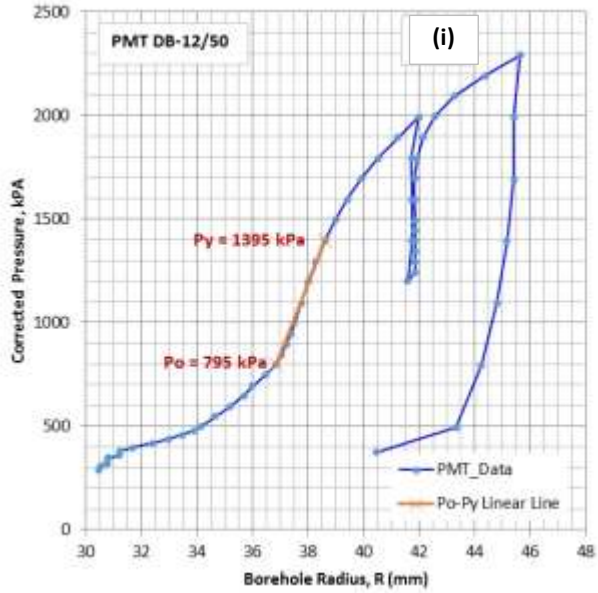

Figure 17. Bad pressuremeter test graph

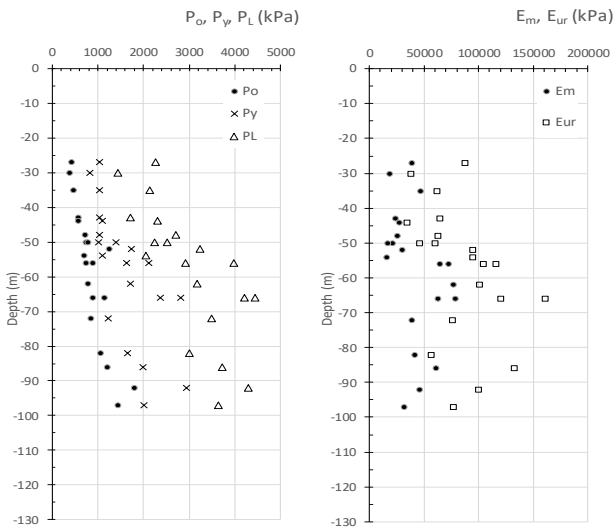

Figure 18. Pressuremeter parameters

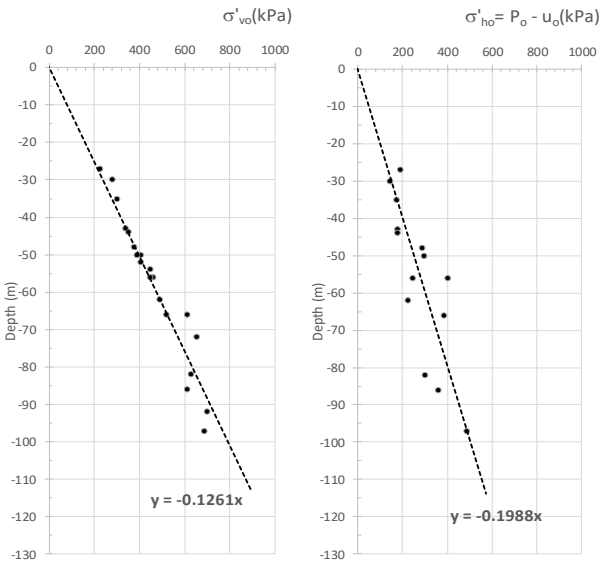

Figure 19. Effective vertical and horizontal pressure (horizontal pressure calculated from Eq. (2))

4. c and ϕ derivation from pressuremeter test

4.1. Mecsi model

Mecsi model as presented by Eq. (8) to (16) was tried to derive the c and ϕ from pressuremeter test data. It was found that Mecsi model could not give a unique values c and ϕ, neither match the test data curve, especially on the plastic phase of the curve, i.e. the part after yield pressure P_y. The typical results are shown in Fig. 20.

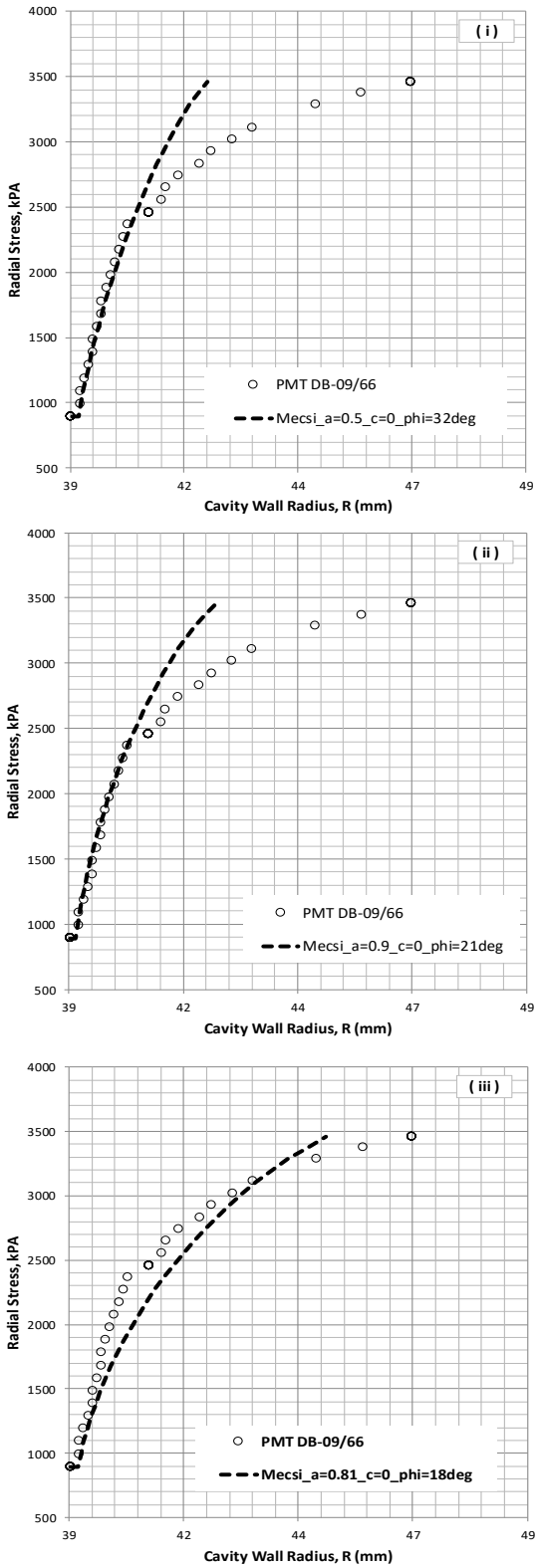

Figure 20. No unique c – ϕ values by Mecsi model

While the test data curve is the same, each of the diagram in Fig. 20 shows different combination of rigidity index and c – ϕ values. The same results were obtained from other test data. It is clear that Mecsi model needs to be investigated further.

4.2. Modified E function model

Through many cycles of numerical study applying the pressuremeter data to cylindrical cavity expansion model proposed by Mecsi, it was found that the key factor lies on changes of deformation modulus with its corresponding stress level as expressed in Eq. (10). Among the parameters in Eq. (10), it is obvious that further investigation need to be carried out on the reference pressure σ_{ref} and rigidity index a. As explained above, Mecsi proposed to use reference pressure of 100 kPa, considering that Mecsi method can only approach the linear part of the pressuremeter curve and far from approaching the plastic part, it looks like the reference pressure σ_{ref}, should be adjusted as follows:

- From P_o to P_y, where the pressuremeter stress-strain or stress-deformation curve still linear, the reference pressure of 100 kPa and a constant value of rigidity index a shall be taken.
- At and above yield pressure P_y, where the curve starts to show non-linear characteristic, the reference pressure shall be taken equal to the yield pressure, i.e. $\sigma_{ref} = P_y$, and rigidity index values needs to be adjusted in accordance with their stress-strain level.

A further trial and error parametric studies was carried out, it was found that at the linear or elastic part of the pressuremeter curve, the rigidity index, a, indeed constant, and the values lies within 0.25 to 0.80 with an average 0.5. However, when entering the non-linear plastic part, apart from changing the reference pressure from 100 kPa to P_y, it appears that Eq. (10) needs to be modified. After many rounds of investigation, rather than doing trial and error, intuitively an idea came to mind to search the changes of plastic deformation modulus through its corresponding strain from within the test data itself. Subsequently, Eq. (10) is then modified to:

- When pressuremeter stress level is still within the linear range, i.e. within P_o to P_y, Eq. (10) becomes:

$$E_s = E_o \left(\frac{\sigma_c}{100}\right)^{0.5} \tag{10a}$$

- When pressuremeter stress level is above yield pressure P_y,

$$E_{sy} = E_{yo}\left(\frac{\sigma_{cy}}{P_y}\right)^{a_{ye}} \rightarrow E_{sy} = m_y E_o \left(\frac{\sigma_{cy}}{P_y}\right)^{a_{ye}} \tag{10b}$$

Where :

E_s = elastic soil deformation modulus at cavity pressure of σ_c

E_o = E_m = pressuremeter modulus as defined in Eq. (4)

E_{sy} = plastic deformation modulus = $\sigma_{cy}/\varepsilon_y$ = cavity pressure at plastic part divided by its corresponding strain (from pressuremeter test data)
E_{yo} = $m_y.E_o = m_y.E_m$
m_y = yield factor
σ_{cy} = cavity pressure at and above yield pressure
a_{ye} = rigidity factor after yield pressure

To find both m_y and a_{ye}, Eq. (10b) then is normalized to:

$$\frac{E_{sy}}{E_m} = m_y \left(\frac{\sigma_{cy}}{P_y}\right)^{a_{ye}} \tag{10c}$$

Then from the pressuremeter data calculate and plot E_{sy}/E_m vs σ_{cy}/P_y, the parameter m_y and a_{ye} can then be obtained by running the power function regression analysis. Fig. 21 shows one of the plotted test data. In this case, $m_y = 0.6151$ and $a_{ye} = -2.06$. Once parameter m_y and a_{ye} are found, substitute these parameters to Eq. (10b).

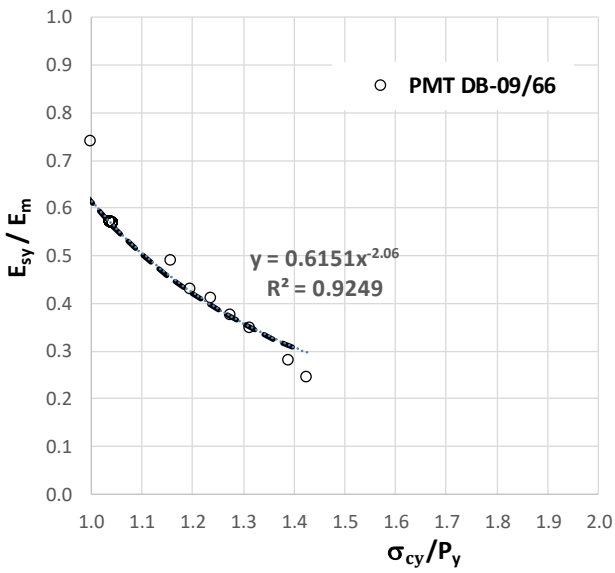

Figure 21. Finding m_y and a_{ye} from pressuremeter test data

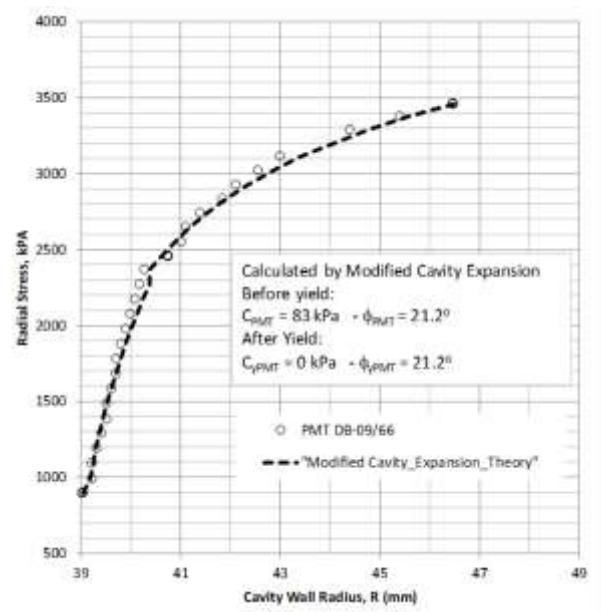

Figure 22. Test data vs modified cavity expansion theory

It is possible to calculate parameter c and ϕ in a more consistent way by using Eq. (8) to (16) but replacing Eq. (10) with Eq. (10a) and (10b). Fig. 22 shows one of the results of pressuremeter test curve matching with curve calculated from the modified E function or modified cavity expansion model. The result shows that when the stiff clay is still in linear "elastic" range, the shear strength consists both cohesion and angle of internal friction (since the parameters are derived from pressuremeter, it is notated as c_{PMT} and ϕ_{PMT}). However, once the soil entering non-linear plastic part, the stiff clay lost its cohesion ($c_{yPMT} = 0$), and only the angle of internal friction remains constant throughout the elastic and plastic phase, i.e. $\phi_{PMT} = \phi_{yPMT}$. The same outcomes are found from all the pressuremeter test.

4.3. Refining with linear hyperbolic model

Due to the manual reading process, the rather fast execution may yield some degreeof erratic readings. Since between P_o and P_y pressuremeter test curve shows linear behaviour, while after P_y the test curve shows hyperbolic characteristics, a rather erratic test curve can be smoothened out with a mathematical approach as follows:

- When pressuremeter stress level is still linear, i.e.within P_o to P_y, the test data can be linearized by linear equation:

  $$\sigma_c = \lambda\, \varepsilon_c + \kappa \tag{17}$$

  where σ_c is cavity wall pressure, ε_c is cavity wall strain, λ and κ is linear line coefficients.

- When pressuremeter stress level is above yield pressure P_y, hyperbolic equation is used:

  $$\sigma_{cy} = \frac{\varepsilon_{cy}}{\alpha + \beta\varepsilon_{cy}} \text{ or } \frac{\varepsilon_{cy}}{\sigma_{cy}} = \alpha + \beta\varepsilon_{cy} \tag{18}$$

  Where σ_{cy} is after yield cavity wall pressure ε_{cy} is after yield cavity wall strain, α and β is hyperbolic coefficients. With this hyperbolic equation, the limit pressure P_L can also be calculated:

  $$P_L = 1/\alpha + P_o \tag{19}$$

Fig. 23 shows the example of smoothing the test data with linear hyperbolic mathematical model.

By smoothing out pressuremeter test data point with linear-hyperbolic model, it is then possible to make a simple program by use of Microsoft Excel spreadsheet to calculate c_{PMT} and ϕ_{PMT} in semi-automatic way. With this method, all the pressuremeter data were re-analysed and the results are shown below.

In Fig. 24 c_{PMT} and ϕ_{PMT} are plotted against the undrained shear strength of the stiff clay obtained from triaxial CIU test. While in Fig. 25 the c_{PMT} and ϕ_{PMT} are plotted against the drained shear strength of the stiff clay obtained from triaxial CIU test.

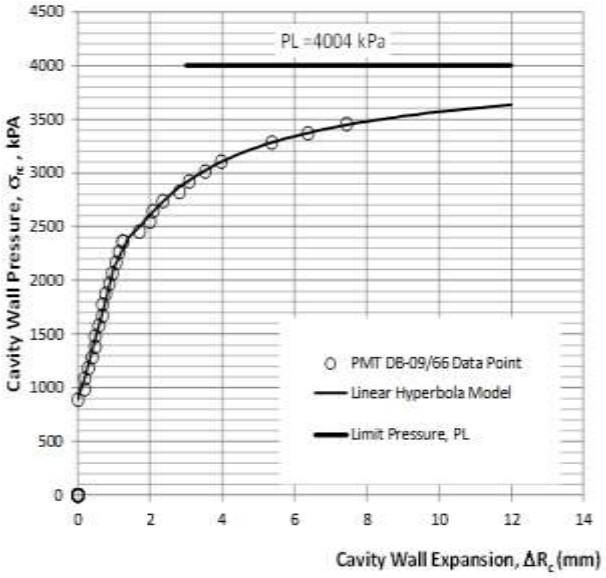

Figure 23. Smoothen out test data using linear hyperbolic mathematical model

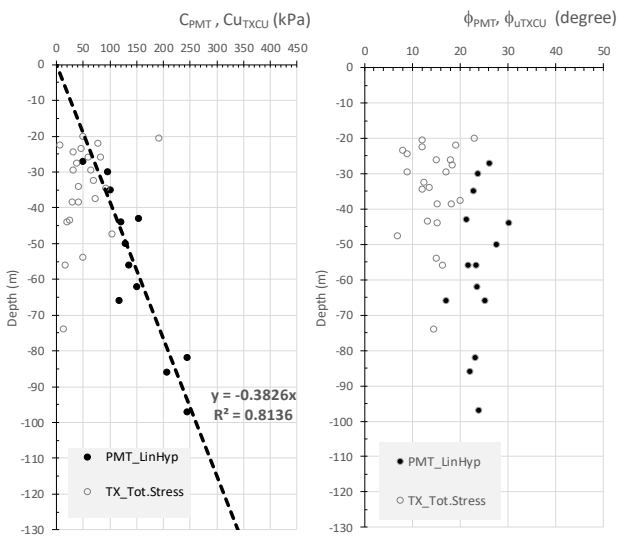

Figure 24. c_{PMT} and ϕ_{PMT} vs triaxial CIU undrained strength

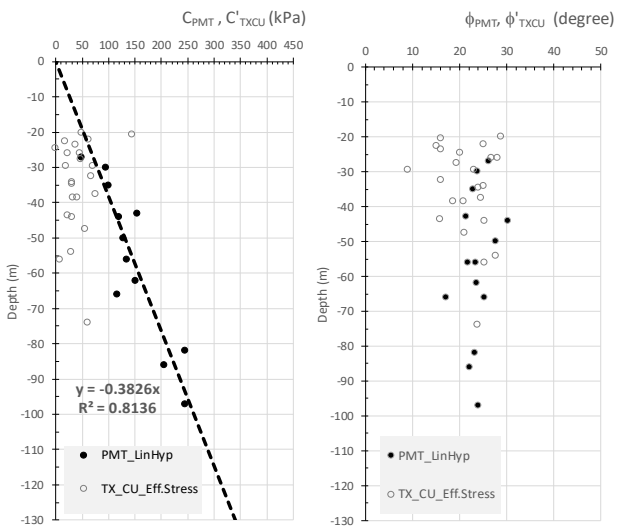

Figure 25. c_{PMT} and ϕ_{PMT} vs triaxial CIU drained strength

5. Undrained shear strength

By employing Gibson and Anderson [11], Marshland and Randolph [12] methods presented in section 2.2.7, undrained shear strength of the stiff clay is derived from the pressuremeter test. Fig. 26 shows example of the derivation with both methods. Results obtained from all the data are plotted in Fig. 27 together with the UU triaxial test data. Gibson and Anderson method undrained shear is 2 – 3 times higher than UU triaxial, while Marshland and Randolph method gives 1.5 times higher undrained shear strength.

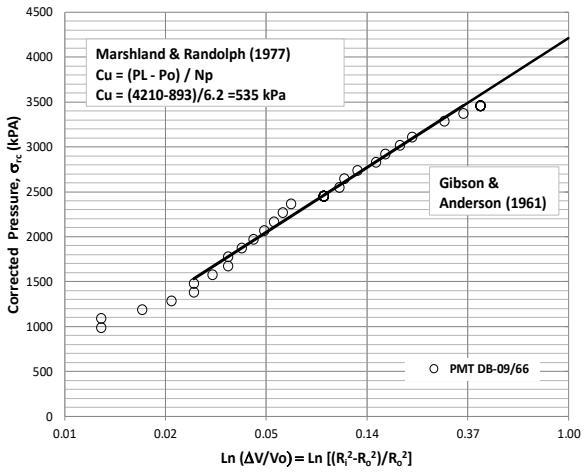

Figure 26. Undrained shear strength derivation from pressuremeter test

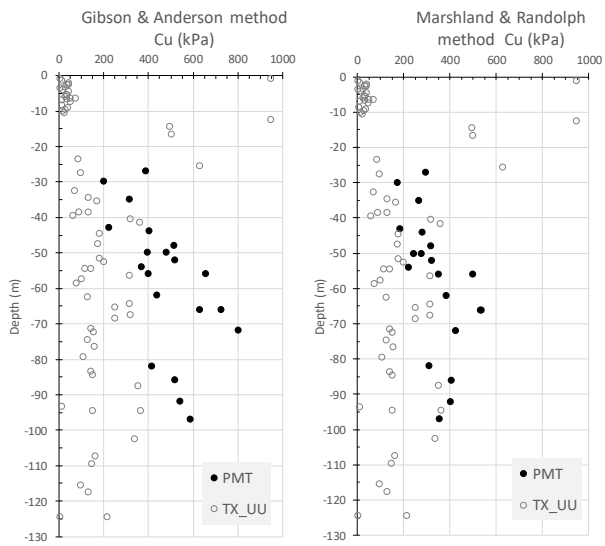

Figure 27. c_{uPMT} vs c_u triaxial UU

6. Discussion

Comparing Fig. 24 and Fig. 25, it can be seen that from 27m to 97m depth the ϕ_{PMT} values are within 20° – 30°. These values fall within the drained angle of internal friction rather than the undrained angle of internal friction. As for the cohesion, the c_{PMT} values have a clear trend increasing with depths, starting from around 50 kPa at 27 m to around 250 kPa at 97m depth, and it is clearly higher than the values obtained from CIU triaxial test, be the undrained or drained cohesion. The lesser values of cohesion from triaxial tests are generally attributed to the

brittle nature of Jakarta cemented stiff clay which tends to have thin hair cracks resulted from the sampling process by thin wall tube sampler and during the preparation of the samples in the laboratory. The higher values of c_{PMT} is due to the cemented nature of the Jakarta stiff clay. Comparing Fig. 25 and Fig. 27, the c_{PMT} values against the corresponding values of c_{uPMT}, it is clear that c_{PMT} values are lower by around 1.5 to 4.0 times the c_{uPMT}. This is consistent with the nature that drained cohesion is lower than undrained cohesion. It can be said that the cohesion values derived from pressuremeter test by modified cavity expansion theory are drained cohesion or at least partially drained cohesion.

Another fact need to mention is that the derivation of shear strength parameters from pressuremeter data by using modified cavity expansion give a clear existence of soil cohesion when the stress strain of the stiff clay is still within the linear "elastic" range, and the stiff clay losses the cohesion once the stress level reaching and above its yield stress level, what remain thereafter is the angle of internal friction which remain constant throughout all the stress level.

From all the above phenomena, it can be concluded or at least postulated that for Jakarta stiff clay, at the initial stage of pressuremeter test the soil is in partially or near drained cohesion, as the radial stress and strain increases and reaches its yield pressure, P_y, the stiff clay is already in fully drained cohesion. The explanation is: at the initial stage, while the radial stress tends to reduce the soil volume, the concurrent induced tangential strain will expand the soil radially, therefore the soil is not in a fully compressive nature, but rather in a radial and tangential ring like shearing nature. Consequently, at this stage the soil at least is in a partially drained condition. At and beyond yield pressure, the induced tangential strain will be large enough to cause the distance within the clay particles move to a larger distance on another to lose its cohesion and left only with its angle of internal friction, at this stage the stiff clay is already in a fully drained condition.

7. Conclusion

From the research, it can be concluded that Mecsi model cannot be directly used to derive the c and ϕ values of Jakarta stiff clay. Its formulation of deformation modulus need to be modified into two parts as written in Eq. (10a) and (10b), with this modified E function, cavity expansion theory can then be applied to derive the shear strength parameters. Pressuremeter test in Jakarta stiff clay initially exhibits partially drained condition and the gradually become fully drained condition when reaching and beyond its yield pressure. The c and ϕ values obtained from pressuremeter test are effective stress parameters. The pressuremeter test can reveal the effect of cementation of Jakarta stiff clay which appear in a higher value of cohesion which cannot be captured by triaxial test due to the difficulty in obtaining a good 'really' undisturbed Jakarta stiff clay samples by normal thin wall tube sampler.

Acknowledgement

The author would like to thank Prof. Paulus P. Rahardjo and Prof. A. Aziz Djajaputra for their continuing and valuable guidance during the research and the preparation of this manuscript. A special acknowledgement also covered to Prof. H. Moeno, R. Karlinasari PhD and S. Herina for their feedbacks.

References

[1] Baguelin, F., Jezeqel, J.F., Lemee, E., and Le Mehaute, A. (1972) "Expansion of Cylindrical Probes in Cohesive Soils", JSMFE, ASCE, Vol. 98; SM11. Proc. Paper 9377, pp1129-1142

[2] Baguelin, F., Jezequel, J.F., and Shields, D.H. (1978) "The Pressuremeter and Foundation Engineering", Trans Tech Publication, Switzerland

[3] Gambin, M. (1980) "A Review of the Menard Pressuremeter over the Last Twenty Years in Europe", Sol Soils, No. 32, Paris

[4] ASTM D4719-00. (2000) "Standard Test Method for Prebored Pressuremeter Testing in Soils", ASTM, 100 Barr Harbor Drive, West Conshohocken, PA 19428-2959, USA

[5] Briaud, J.L. (2013) "Geotechnical Engineering: Unsaturated and Saturated Soils", John Wiley & Sons, New Jersey, USA

[6] Clayton, R.I., Simons, N.E., and Matthews, M.C. (1982) "Site Investigation A Handbook for Engineers", Granada Publishing, London

[7] Briaud, J.L. (1992) "The Pressuremeter", A.A. Balkema, Rotterdam

[8] Clarke, B.G. (1995) "Pressuremeters in Geotechnical Design", Blackie Academic and Professional, London

[9] Gouw, Tjie-Liong (1984) "A Study on Ménard dan Oyo Pressuremeter and Its Application in Estimating Bearing Capacity of Soils", an undergraduate thesis, Civil Engineering Division, Universitas Katolik Parahyangan, Bandung

[10] Ghionna, v., et al. (1981), "Performance of Self-boring Pressuremeter Tests in Cohesive Deposits", Report FHWA/RD-81/173/1981, MIT, Boston

[11] Gibson, R.E., and Anderson, W.F. (1961) "In Situ Measurement of Soil Properties with the Pressuremeter", Civil Engineering and Public Works Review, Vol 56, pp615-618

[12] Marsland, A. and Randolph, M.F. (1977) "Comparisons of the Results from Pressuremeter Tests and Large in Situ Plate Tests in London Clay", Geotechnique, June 1977 27(2), pp.217-243

[13] Mair, R.J. and Wood, D.M. (1987), Pressuremeter Testing Methods and Interpretation, Butterworths, London

[14] Windle, D. and Wroth, C.P. (1977a) "The Use of Self-boring Pressuremeter to determine the Undrained Properties of Clays", Ground Engineering, Sept 1977 10(6), pp.37-46, London

[15] Windle, D. and Wroth, C.P. (1977b), "In-situ Measurement of the Properties of Stiff Clays", Proceeding of 9th International Conference on Soil Mechanics and Foundation Engineering, Tokyo, Vol. 1, pp.347-352

[16] Hughes, J.M.O, Worth, C.P., and Windler, D. (1977) "Pressuremeter tests in Sands", Geotechnique, Vol 27 (4): p. 455-477

[17] Fahey, M. and Randolph, M.F. (1984) "Effect of Disturbance on Parameters Derived from Self-boring Pressuremeter Tests in Sand", Geotechnique, March 1984, 34 (1) pp. 81-87

[18] Schnaid, F. (2009) "In Situ Testing in Geomechanics", Taylor and Francis, London

[19] Bruzzi, D. et al (1986) "Self-boring Pressuremeter in Po River Sand", in The Pressuremeter and its Marine Applications, American Society for Testing and Materials, Philadelphia, Special Publication STP 950, 1986

[20] Gambin, M. (1995) "Reasons for the Success of Menard Pressuremeter", Proceedings of Fourth International Symposium on Pressuremeters, May 17-19, 1995, Sherbrooke, Quebec, Canada

[21] Boumedi, J.Y., Baud, J.P. and Radiquet, B. (2009) "LNG Tanks at Damietta on Drilled Shafts Designed and Tested Using Menard PMT", Foundation Design with Menard Pressuremeter Test, French Contributions to International Foundation Conggress & Equipment, Expo '09, p. 35-42; also in ASCE Geotechnical Special Pu Bustamante, M., Gambin, M., and Gianeselli, L. (2009) "Pile Design at failure Using the Menard Pressuremeter: an Up-Date", Foundation Design with Menard Pressuremeter Test, French Contributions to International Foundation Conggress &

Equipment, Expo ’09, p. 11-18; also in ASCE Geotechnical Special Publication no. 186, pp.127-134blication no. 186, pp.103-110
[22] Bustamante, M., Gambin, M., and Gianeselli, L. (2009) “Pile Design at failure Using the Menard Pressuremeter: an Up-Date”, Foundation Design with Menard Pressuremeter Test, French Contributions to International Foundation Conggress & Equipment, Expo ’09, p. 11-18; also in ASCE Geotechnical Special Publication no. 186, pp.127-134
[23] Gambin, M. and Frank, R. (2009) “Direct Design Rules for Piles using Menard Pressuremeter Test”, Foundation Design with Menard Pressuremeter Test, French Contributions to International Foundation Conggress & Equipment, Expo ’09, p. 3-10; also in ASCE Geotechnical Special Publication no. 186, p.111-118
[24] Reiffsteck, P. (2009) “ISP5 Pile Prediction Revisited”, Foundation Design with Menard Pressuremeter Test, French Contributions to International Foundation Conggress & Equipment, Expo ’09, p. 11-18; also in ASCE Geotechnical Special Publication no. 186, pp.50-57
[25] Schlosser, F., Guilloux, A., Zaghouani, K. and Berthelot, P. (2009) “Rades Bridge Drilled Shafts Designed and Tested Using Menard Pressuremeter”, Foundation Design with Menard Pressuremeter Test, French Contributions to International Foundation Conggress & Equipment, Expo ’09, p. 27-34; also in ASCE Geotechnical Special Publication no. 186, pp.42-49
[26] Hamidi, B., Debats, J.M., Nikraz, H., and Varaksin, S. (2013) “Offshore Ground Improvement Records”, Australian Geomechanics Journal, Vo. 48 No. 4 Dec 2013, p.111-122
[27] Briaud, J.L., Pacal, A.J, dan Shively, A.W. (1984) “Power Line Foundation Design Using the Pressuremeter”, Proceeding of First International Conference on Case Histories in Geotechnical Engineering, p.279-283, Missouri, USA
[28] Jefferies, M.G. (1988) “Determination of Horizontal Geostatic Stress in Clay with Self Bored Pressuremeter”, Canadian Geotechnical Journal, Vol 25, pp. 559-573
[29] Ferreira, R.S. and Robertson, P.K. (1991), “Interpretation of Undrained Self-boring Pressuremeter Test Results Incorporating Unloading”, Canadian Geotechnical Journal, Oct. 1991
[30] Briaud, J.L. (1997) “SALLOP: Simple Approach for Lateral Loads on Piles”, Journal of Geotechnical and Geoenvironmental Engineering, p.958-964
[31] Bullock, P.J. (2004) Insitu Rock Modulus Apparatus, Report on Contract No. BC-354-RPWO No. 13, submitted to Florida Department of Transportation, 23 August 2004
[32] Silvestri, D. and Ghassan, A.S. (2012) “Analytical Solution for Undrained Plane Strain Expansion of a Cylindrical Cavity in Modified CamClay”, Geomechanics and Engineering, Vol. 4, No. 1 (2012), p. 19-31
[33] Ramdane, B., Nassima, A. and Quarda, B. (2016) “Interpretation of a Pressuremeter Test in Cohesive Soils”, Proceedings of International Conference on Geotechnical Engineering, 21-23 Feb 2013, Tunisia
[34] Mecsi, J. (2013) “Geotechnical Engineering Examples and Solutions Using the Cavity Expanding Theory”, Hungarian Geotechnical Society, Hungary
[35] Ladanyi, B. (1961) “Etude Theorique at Experimentale de l’expansion daus un Sol Pulverulent d’une cavite Presintant une Synietrie Spherique ou Cylindrique”, Annaes de Travaux Publics de Belgique; Buxelles No. 2 et 4
[36] Vesic, A.S. (1972, “Expansion of Cavities in an Infinite Soil Mass”, JSMFE, ASCE, Vol. 98, SM3, Proc. Paper 8790, pp.265-290
[37] Vesic, A.S. (1975) Principles of Pile Foundation Design, Soil Mechanics Series No 38, Duke University, N.C
[38] Baligh, M.M. (1976) “Cavity Expansion in Sands with Curved Envelopes”, JSMFE, ASCE: Poc. Paper 12536, p.1131-1146
[39] Wroth, C.P. and Windle, D. (1975) “Analysis of Pressuremeter Test Allowing for Volume Change”, Geotechnique, Vol 25, No.3, Technical Notes, pp.598-604
[40] Datye, K.R. and Nagraju, S.S. (1977) “Reinforce Granular Columns – A New Design Approach”, Proceeding of IX ICSMFE, Tokyo, Special Session No. 10
[41] Pandit, N.S., Chaney, R.C. and Fang H.Y. (1983) Review of Cavity Expansion Models in Soil and Its Applications, Fitz Engineering Laboratory, Department of Civil Engineering, Lehigh University, Bethlehem, Pennsylvania, USA
[42] Yu, H.S. (2000), Cavity Expansion Methods in Geomechanics, Springer Science Business Media B.V., NewCastle, Australia